Supplementary Information

Anchored Phosphatases Modulate Glucose Homeostasis

Simon A. Hinke, Manuel F. Navedo, Allison Ulman, Jennifer L. Whiting, Patrick J. Nygren, Geng Tian, Antonio J. Jimenez-Caliani, Lorene K. Langeberg, Vincenzo Cirulli, Anders Tengholm, Mark L. Dell'Acqua, L. Fernando Santana and John D. Scott

Inventory of supplementary information:

Supplementary figures (6)

Supplementary figure legends

Supplementary materials and methods

Supplementary references

Supplementary Figure S1 Characterization of AKAP150 and AKAP220 effects in INS-1 cells, and biochemical and hormone analysis of AKAP150KO mice. (**A**) Digoxigenin-RII overlay of INS-1(832/13) input lysate (lane 1), and immunoprecipitated AKAP150 using rabbit polyclonal antisera (lane 3). Control immunoprecipitation with rabbit IgG was used to observe the background (lane 2). Data indicate the ability of AKAP150 to bind PKA-RII, defining it as an AKAP, and that it is expressed in insulinoma tissue. (**B**) Digoxigenin-RII overlay of INS-1(832/13) input lysate (lane 1), and immunoprecipitated AKAP220 using rabbit polyclonal antisera (lane 3). Control immunoprecipitation with rabbit IgG was used to observe the background (lane 2). Data indicate the ability of AKAP220 to bind PKA-RII, defining it as an AKAP, and that it is expressed in insulinoma tissue. (**C**) Densitometry quantification of AKAP150 gene silencing for hormone secretion studies (Figure 1C-E and Supplementary Figure 1D & E). Immunoblot analysis was performed for each secretion experiment (representative blot shown in Figure 1C), probed for AKAP150 and tubulin as a loading control, and quantified using ImageJ software. (**D**) Glucose- and (**E**) Forskolin-stimulated growth hormone release from INS-1(832/13) cells co-transfected with human growth hormone (pFOX.hGH.CMV) and pSilencer with (p150i) or without (Control) rat specific AKAP150 shRNA sequence described in (Hoshi *et al*, 2005). (**F**) Representative immunoblot showing knock-down of AKAP220 using siRNA (Dharmacon) in transfected INS-1(832/13) cells. (**G**) Amalgamated densitometry quantification of AKAP220 protein levels for INS-1(832/13) cells used for hormone secretion experiments in cells transfected with AKAP220 or control siRNA. (**H**) Growth hormone secretion from INS-1(832/13) cells co-transfected with pFOX.hGH.CMV and RISC-Free siRNA control or AKAP220i (duplex 2) in response to glucose and GLP-1. (**I**) Growth hormone secretion from INS-1(832/13) cells co-transfected with pFOX.hGH.CMV and RISC-Free siRNA control or AKAP220i (duplex 2) in response to 20mM glucose with 10μM forskolin. (**J**) Expression level of hGH in transfected INS-1(832/13) cells. (**K**)

Immunoprecipitation of AKAP150 from brain lysate showing co-precipitation of PKA-RII and PP2B from WT mice but not AKAP150KO, where AKAP150 protein is absent. (**L**) Enrichment of PKA-RII by cAMP-agarose affinity chromatography from WT and AKAP150KO brain lysates indicates AKAP150 co-purifies from WT mice but not AKAP150KO, where AKAP150 protein is absent. Ethanolamine-agarose was used as a control. (**M**) Calmodulin-agarose directly binds to and enriches AKAP150 from WT brain lysate and co-purifies PKA-RII, but not in AKAP150KO lysates where the protein is absent. Ethanolamine-agarose was used as a control. (**N**) Immunoblot probing transformed mouse β-cell (MIN6) and α-cell (αTC1-6) lines for AKAP150, PKA-RII and GAPDH. (**O**) Plasma insulin concentrations measured from fasted wildtype and AKAP150KO mice and following IP glucose (1.5g/kg) injection. Immunoblot data are representative of 3 independent experiments. Data represent mean±SEM. *p≤0.05.

Supplementary Figure S2 Analysis of WT and AKAP150KO mouse pancreatic islet function. (**A**) Analysis of islet preparation viability and ability to catabolize glucose using the MTT assay. (**B**) Integrated dynamic insulin secretory responses to glucose and (**C**) forskolin for islet perifusion data presented in Figure 2B. (**D**) Capacitance was used to distinguish dissociated β-cells from non-β-cells by virtue of size, as described (Braun *et al*, 2004). Cells were selected in this manner for use in electrophysiological experiments presented in Figure 2C-E. (**E**) Quantitative real time PCR was used to compare WT and AKAP150KO islet mRNA expression for K_{ATP} channel and L-type Ca^{2+} channel subunits, as described in the Experimental Procedures section. Data represent mean±SEM. *p≤0.05.

Supplementary Figure S3 Metabolic profiling of WT and AKAP150KO mice. (**A**) Area under the curve (AUC) of IP glucose (1.5g/kg) tolerance test glycemic excursions over 90min shown in Figure 3A. (**B**) Fasting and fed plasma insulin concentrations from WT and AKAP150KO

mice. Data show blood insulin levels are significantly reduced in AKAP150 null mice in the fasted state, but not during the fed state. (**C**) Fed circulating C-peptide levels from WT and AKAP150KO mice. (**D**) Fed plasma glucagon concentrations from WT and AKAP150KO mice. (**E**) Fed plasma glucagon-like peptide-1 (GLP-1) concentrations from WT and AKAP150KO mice. (**F**) Fed plasma glucose-dependent insulinotropic polypeptide (GIP) concentrations from WT and AKAP150KO mice. Quantitative real time PCR was used to compare WT and AKAP150KO gastrocnemius (**G**) and liver (**H**) mRNA expression for G6Pase and PEPCK, as described in the Experimental Procedures section; G6Pase was present at very low levels in skeletal muscle, but was still included in the analysis. (**I**) Immunoprecipitation of gastrocnemius muscle IRS-1 after saline or 1.0U/kg recombinant insulin injection. 4mg protein extract in RIPA with phosphatase and protease inhibitors was incubated overnight with 2 μg mouse anti-IRS-1 antibody (Millipore), cleared by centrifugation, and immune complexes purified with Protein G-sepharose (Upstate). Immunoblot analysis was performed with rabbit anti-IRS-1 (Abcam) or rabbit anti-(P)Ser612-IRS-1 (Cell Signaling). Densitometry of results from 3 animals per genotype are shown in (**J**). Data represent mean±SEM. *p≤0.05.

Supplementary Figure S4 Metabolic profiling of control (*AKAP150$^{fl/fl}$*) and AKAP150βKO (*AKAP150$^{fl/fl}$/Ins2-Cre+/-*) mice. (**A**) Area under the curve (AUC) of IP glucose (1.5g/kg) tolerance test glycemic excursions over 90min shown in Figure 4E.

Supplementary Figure S5 Additional characterization of AKAP150Δ36 mice. (**A**) Enrichment of PKA-RII by cAMP-agarose affinity chromatography from WT and AKAP150Δ36 brain lysates indicates AKAP150 co-purifies only from both WT mice, but not from mice where the PKA binding domain of AKAP150 has been deleted. Ethanolamine-agarose was used as a control.

(**B**) Calmodulin-agarose directly binds to and enriches AKAP150 from WT and AKAP150Δ36 brain lysate and co-purifies PKA-RII from both genotypes. The N-terminal CaM binding domain of AKAP150 is not altered by C-terminal deletion of the last 36 amino acids of the scaffold. Ethanolamine-agarose was used as a control. (**C**) Integrated dynamic insulin secretory responses to glucose and (**D**) forskolin for islet perifusion data presented in Figure 5G. (**E**) Area under the curve (AUC) of IP glucose (1.5g/kg) tolerance test glycemic excursions over 90min shown in Figure 4H. (**F**) Immunoblot analysis of active (P)Thr^{172}-AMPK, total AMPK, and GAPDH from skeletal muscle homogenates from WT and AKAP150Δ36 mice. Two biological replicates are shown for each genotype and condition. Quantification of compiled results was performed by densitometry analysis of active (P)Thr^{172}-AMPK normalized to total respective protein level (**G**). Immunoblot data are representative of 3 independent experiments; densitometry represents results from 3 individual animals of each genotype. Data represent mean±SEM. *p≤0.05.

Supplementary Figure S6 Additional characterization of AKAP150ΔPIX mice. (**A**) Enrichment of PKA-RII by cAMP-agarose affinity chromatography from WT and AKAP150ΔPIX brain lysates indicates AKAP150 co-purifies from both WT and AKAP150ΔPIX mice. Results indicate that deletion of the PIAIIIT motif from AKAP150 does not alter its ability to bind PKA-RII. Ethanolamine-agarose was used as a control. (**B**) Calmodulin-agarose directly binds to and enriches AKAP150 from WT and AKAP150ΔPIX brain lysate and co-purifies PKA-RII from both genotypes. The N-terminal CaM binding domain of AKAP150 is not altered by deletion of the PIAIIIT motif. Ethanolamine-agarose was used as a control. (**C**) Integrated dynamic insulin secretory responses to glucose and (**D**) forskolin for islet perifusion data presented in Figure 6G. (**E**) Area under the curve (AUC) of IP glucose (1.5g/kg) tolerance test glycemic

excursions over 90min shown in Figure 6H. (**F**) Immunoblot analysis of active (P)Thr^{172}-AMPK, total AMPK, and GAPDH from skeletal muscle homogenates from WT and AKAP150ΔPIX mice. Two biological replicates are shown for each genotype and condition. Quantification of compiled results was performed by densitometry analysis of active (P)Thr^{172}-AMPK normalized to total respective protein level (**G**). Immunoblot data are representative of 3 independent experiments; densitometry represents results from 3 individual animals of each genotype. Data represent mean±SEM. *p≤0.05.

Supplementary Materials and Methods

Experimental Animals

All animals were housed at the University of Washington, Seattle, under a 12h light/dark cycle with free access to food (LabDiet 5001) and water. All procedures were approved by the institutional IACUC review process. Animals were maintained on a C57Bl/6 (Jackson Laboratories; backcrossed 4-8 generations); experiments were performed on littermate or age-matched mice from het X het breeding pairs, or age-matched mice from F1 homozygous crosses. Generation of global AKAP150 (Tunquist *et al*, 2008) and AKAP150Δ36 (Weisenhaus *et al*, 2010) mice have been previously described. AKAP150ΔPIX mice were developed in conjunction with the Rocky Mountain Neurological Disorders Transgenic and Gene Targeting Vectors Core and housed in the University of Colorado Anschutz Medical Campus Center for Comparative Medicine. Briefly, the AKAP150ΔPIX mutation, which removes the conserved PIAIIIT motif (amino acids 655-661), was introduced into the single AKAP150 coding exon 2 in the *AKAP5* gene by homologous recombination in C57Bl6Jx129 F1 embryonic stem cells with a loxP-flanked neomycin cassette located downstream of the exon. Targeted ES clones were identified by G418 selection for the neomycin resistance gene and PCR-screening of genomic DNA, expanded, and injected into blastocysts that were implanted

into surrogate females. Heterozygous and homozygous mice carrying the mutation were derived from the resulting F0 chimeric founders by standard breeding with C57BL/6J. AKAP150ΔPIX mice housed in a home-cage environment have no obvious phenotypic alterations in body weight, life-span, breeding, or behavior. A full description of the AKAP150ΔPIX knock-in targeting vector and additional characterization of AKAP150ΔPIX mice will be published elsewhere (Dell'Acqua *et al*, in preparation). Ins2-Cre mice (Postic *et al*, 1999) on a pure C57Bl/6J background were obtained from the Jackson Laboratories. Transgenic mice containing two LoxP sites flanking the AKAP150 coding exon ($AKAP150^{fl/fl}$) (Tunquist *et al*, 2008) were backcrossed onto the Ins2-Cre background to produce *$AKAP150^{fl/fl}$/Ins2-Cre+/-* mice to produce mice lacking AKAP150 expression in tissues that normally express insulin.

Cell Culture and Islet Isolation

Rat INS-1(832/13) insulinoma cells were cultured as described (Hohmeier *et al*, 2000) in RPMI-1640, 10% FBS, 10mM HEPES, 2mM glutamine, 1mM sodium pyruvate, 50μM β-mercaptoethanol and antibiotics (Invitrogen). For transfection experiments, $3x10^6$ cells were seeded into 10cm dishes (Falcon) and incubated for 2 days; transfection was achieved using Lipofectamine2000 and OptiMEM for 4h as per the supplied protocol (Invitrogen). Plasmids used were pSilencer (Ambion) or the previously described pSilencer with a rat specific AKAP150 targeted shRNA insert (Hoshi *et al*, 2005), siGENOME RISC-Free siRNA control (Dharmacon D-001220-01) or rat AKAP220 siRNA duplex 2 (Dharmacon D-090987-02), human growth hormone (pFox.hGH.CMV) (Goldfine *et al*, 1997), and pEGFP (Invitrogen). 5μg hGH plasmid and 0.5μg pEGFP plasmids were included in each transfection, to measure secretion from transfected cells and to assess transfection efficiency; siRNA or pSilencer

vector with or without targeting insert was included to bring the DNA/RNA transfected to a total of 10μg per 10cm dish. Transfected cells recovered overnight, were subcultured into 24-well plates (Falcon) at $5x10^5$ cells/well and cultured for another 48h before use in secretion experiments.

Collagenase P (Roche) digested pancreatic islets were isolated as previously described (Delmeire *et al*, 2003; Hansotia *et al*, 2004) by handpicking under a stereo microscope. Islets were cultured in suspension overnight in RPMI supplemented with 10% FBS, 10mM HEPES, 1mM sodium pyruvate, and antibiotics, prior to re-picking healthy islets for experiments.

Immunoprecipitation, Western Blotting and Tissue Analysis

Cultured cells and mouse tissues were homogenized in lysis buffers according to the experiments performed: RIPA buffer for immunodetection, immunoprecipitation buffer (0.5% NP-40, 100mM NaCl, 50mM Tris-HCl, pH7.4), or phosphatase inhibitor buffer (1% Triton X-100, 60mM β-glycerophosphate, 20mM MOPS, 5mM EDTA, 5mM EGTA, 1mM Na_3VO_4, 20mM NaF, pH7.2), each with protease inhibitors added (1mM benzamidine, 10μM AEBSF, 25μg/mL leupeptin). Lysates were prepared by sonication (cells) or Polytron homogenization (tissues) for 60s on ice, prior to refrigerated centrifugation to remove insoluble material. Immunoprecipitation was performed for 2h at 4°C in the presence of 25μL protein A-agarose beads (Upstate), 2μg antibody, and 1mL of lysate diluted to ~1mg/mL. Immune complexes were washed thrice in IP buffer and bound proteins eluted by boiling in 2X NuPage sample buffer with 0.5M DTT (Invitrogen), and resolved by SDS-PAGE (Invitrogen NuPage). This method was also adapted to cAMP-agarose (BioLog) and calmodulin-agarose (Sigma). Conventional Western blotting was performed by loading 50μg/lane, electrophoretic separation, transfer to nitrocellulose, and blocking in 1X Blotto. Protein concentrations were determined

using the Micro BCA Protein Assay kit (Pierce). Primary antibodies used in this report are: rabbit anti-AKAP150 (V088; (Efendiev *et al*, 2010)), goat anti-AKAP150 (C-20; Santa Cruz), rabbit anti-AKAP220 (Logue *et al*, 2011), mouse anti-RIIα (clone 40; BD Signal Transduction), mouse anti-E-Cadherin (BD Signal Transduction), guinea pig anti-insulin (Dako), rabbit anti-glucagon (Dako), mouse anti-α-tubulin (clone B-5-1-2), anti-GAPDH (clone 71.1; Sigma), rabbit anti-(P)Thr^{173}-AMPKα (clone 40H9), rabbit anti-AMPKα, rabbit anti-(P)Ser^{473}-Akt1 (Cell Signaling), rabbit anti-Akt1 (Upstate), mouse anti-IRS-1 (Millipore), rabbit anti-IRS-1 (Abcam), rabbit anti-(P)Ser^{612}-IRS-1 and mouse anti-PP2B$_B$ (clone CN-B1; Abcam). Digoxigenin-labelled PKA-RIIα for use in far Western RII overlays has been previously described (Logue *et al*, 2011). Secondary antibodies used were from Abcam (HRP-anti-digoxigenin), GE Healthcare (HRP-anti-rabbit and -mouse IgG) and eBioscience (Mouse Trueblot HRP-anti-mouse IgG).

Total pancreatic insulin content was measured as previously described (Pamir *et al*, 2003). Pancreata were harvested from fed mice, Polytron homogenized (30sec) on ice in 5mL cold 2N acetic acid, boiled for 5min, transferred to ice, centrifuged for at 15000g at 4°C for 15min. Supernatant extract was analysed for protein content (BCA assay, Pierce) and insulin content (ELISA, Millipore).

For AKAP150 staining, paraffin sections from 10% neutral buffered formalin fixed pancreas of 18 week-old WT or AKAP150KO mice were first deparaffinised with Citrisolv, rehydrated and then subjected to antigen retrieval with a citrate buffer solution pH8. Following blocking in PBS containing 1% BSA, 2% donkey serum, and 50mM Glycine for 1 hour at room temperature, sections were incubated with primary antibodies for 4 hours at room temperature. In order to enhance antibody-specific immunoreactivity a biotin-conjugated donkey anti-goat antibody was then applied to the sections and incubated for 45 minutes. After washing in PBS (0.1% BSA, 0.2% donkey serum), sections were then incubated for another 45 minutes with a

cocktail of fluorophore-conjugated secondary antibodies (FITC-donkey anti-biotin; Rhodamine-donkey anti-guinea pig; Cy5-donkey anti-mouse). Stained sections were then mounted and imaged on a Nikon *Eclipse* 90*i* fluorescence microscope (Nikon Inc. USA).

To measure islet area and β-cell mass, pancreata from WT, AKAP150KO, AKAP150Δ36, and AKAP150ΔPIX (3 animals of each) were fixed and paraffin embedded as above, after measurement of their wet weights; tissue blocks were coded to permit blinding of the experiment. 4 serial sections were taken at 200 μm intervals throughout each tissue block, and co-stained for insulin (blue), glucagon (green) and E-cadherin (red), or IgG controls. Secondary antibodies used were FITC-donkey anti-guinea pig, rhodamine-donkey anti-rabbit and Cy5-donkey anti-mouse, all from Jackson Immuno Research. 10X immunofluorescence images of entire tissue slice at each depth were captured as above and analyzed with NIS-Elements AR 3.2 software to measure islet area as a percentage of total pancreatic area. β-cell mass was calculated using the wet weights of the dissected pancreata.

For examination of phospho-AMPK and phospho-Akt in skeletal muscle and liver samples, mice were fasted overnight, and injected with either saline or 1.0U/Kg recombinant human insulin (HumulinR; Eli Lilly). After 15min, animals were sacrificed by cervical dislocation and the liver and gastrocnemius muscles briefly rinsed in ice cold phosphate buffered saline (PBS) and snap frozen in liquid nitrogen. Tissues were homogenized in phosphatase and protease inhibitor containing solubilization buffer as described above, prior to protein assay and immunoblot analysis. For examination of phospho-IRS-1 in skeletal muscle extracts, the experiment proceeded as above, but tissues were instead homogenized in RIPA buffer with phosphatase and protease inhibitors. 4mg of protein extract was incubated overnight with 2 μg mouse anti-IRS-1 antibody (Millipore), cleared by centrifugation, and immune complexes

purified with Protein G-sepharose (Upstate) prior to immunoblot analysis. Densitometry was performed using NIH ImageJ software (v10.2).

Hormone Secretion Studies

INS-1(832/13) cells transfected with hGH and gene silencing vectors or siRNA were washed twice with 37°C HEPES-buffered Kreb's ringer bicarbonate buffer (KRBH; mM: 25 HEPES, 5 $NaHCO_3$, 1.2 $MgSO_4$, 1.2 KH_2PO_4, 4.74 KCl, 125 NaCl, 1 $CaCl_2$) with 2mM glucose, and pre-incubated 1h at 37°C/5%CO_2. Media was replaced with 1mL of KRBH with 2 or 20mM glucose, with or without GLP-1 (Bachem) or forskolin (Sigma), and incubated for 1h. Supernatants were collected, centrifuged, and stored at -20°C until hGH or insulin was measured by ELISA (Roche or Millipore, respectively) according to the manufacturer's instructions.

Static insulin release experiments from overnight cultured primary islets were performed as per Pamir *et al* (Pamir *et al*, 2003). Size matched islets (~70-300 μm in diameter) were re-picked at 15 islets per tube in triplicate, and pre-incubated in 2mM glucose containing RPMI with 10mM HEPES and 0.1% BSA (Sigma) for 45min at 37°C. Tubes were gently centrifuged and media replaced with stimuli: 2, 8, 15mM glucose, with or without 10μM forskolin, and incubated an additional 45min. Tubes were chilled on ice, centrifuged (1200rpm/4°C/5min), and a sample of supernatant was removed for insulin determination. The remaining media and islet pellet were acidified with glacial acetic acid and sonicated for normalization purposes. Islet perifusion was performed as described on re-picked overnight-cultured islets (100 per chamber) sandwiched in Biogel P2 (BioRad) (Delmeire *et al*, 2003; Hansotia *et al*, 2004). Islets were pre-perifused with 37°C 2mM RPMI/10mM HEPES/0.1% BSA continuously bubbled with carbogen, at a flow rate of 0.5mL/min for 20min. Subsequently, fractions were collected at 1min intervals while perifusion solution was changed to contain 11 or 20mM glucose with or without 10μM forskolin. At the conclusion of the experiment, islets were

extracted in 2N acetic acid with 0.25% BSA with sonication for normalization. Insulin was measured using mouse insulin-specific ELISA kits from Millipore or Alpco as according to included instructions.

In Vivo Metabolism Studies

Glucose tolerance tests were performed on mice following overnight food deprivation. Conscious mice were injected with 1.5g/Kg glucose (10%w/v; Sigma) into the intraperitoneal cavity after basal samples were obtained. Blood glucose was measured from tail vein samples using a handheld glucometer (OneTouch Ultra, LifeScan) at the times indicated in the figures over a 90min period. For plasma hormone determination, whole blood was collected from the tail vein using heparinized capillary tubes (Fisher), and plasma separated by refrigerated centrifugation. Samples were stored at -20°C until hormone measurement by commercial ELISA kits: ultrasensitive mouse insulin (CrystalChem), glucagon (Yanaihara), GLP-1 (Alpco), and GIP (Millipore). The pyruvate tolerance test was performed identically to the IP glucose tolerance test, but substituting sodium pyruvate (10%w/v; Sigma), and tracking the appearance of glucose into the circulation. Insulin tolerance testing was performed on matched fed mice injected with 0.5U/Kg recombinant human insulin (HumulinR, Eli Lilly); the decrease in blood glucose from baseline was monitored by tail vein whole blood samples. The glucagon tolerance test was performed by injecting fed mice with 25nmol/Kg synthetic glucagon (Bachem) dissolved in 0.9% saline into the IP space, and measuring the release of glucose into the blood stream.

Isolated Islet Studies

The viability and metabolism of overnight-cultured collagenase isolated islets was determined by the 3-(4,5-dimethylthiazolyl-2)-2,5-diphenyltetrazolium bromide (MTT) assay, as previously

described (Hinke *et al*, 2007; Janjic & Wollheim, 1992). Briefly, islets were re-picked into microcentrifuge tubes in triplicate and washed twice in 2mM glucose KRBH. Following a 30min pre-incubation in the same buffer at 37°C, media was changed to KRBH containing 2, 11, or 20mM glucose and 0.5mg/mL MTT (Sigma), and incubated for 2h/37°C. Following centrifugation (3000rpm/4°C/10min) and removal of the supernatant, formazan crystals were dissolved in DMSO and absorbance read at A_{562} and A_{690}.

Ca^{2+} currents in β-cells were examined using the whole-cell configuration of the patch-clamp technique with an Axopatch 200B. Isolated islets were dispersed into single cells by trypsin/EDTA (Invitrogen) digestion, and cultured overnight on poly-lysine coated glass coverslips. During experiments, cells were continuously superfused with a solution composed of (in mM): 138 NaCl, 5.4 KCl, 1 $MgCl_2$, 10 $CaCl_2$, 2 Glucose, and 10 HEPES adjusted to pH 7.4. Pipettes were filled with a solution with the following constituents (in mM): 87 Cs-aspartate, 20 CsCl, 1 $MgCl_2$, 5 MgATP, 10 HEPES, and 10 EGTA adjusted to pH 7.2 with CsOH. A voltage error of 10 mV attributable to the liquid junction potential of these solutions was corrected for offline. Whole-cell, nifedipine-sensitive, L-type Ca^{2+} currents were sampled at 20 kHz and were low-pass filtered at 2 kHz.

Current-voltage relationship of nifedipine-sensitive Ca^{2+} currents was obtained from cells depolarized for 200 ms from the holding potential of -70 mV to voltage ranging from -70 mV to +70 mV. The voltage dependence of activation was obtained from peak I_{Ca} currents at test potentials between -70 to +10 mV. These peak currents were converted into conductance (G = I_{Ca} / [test pulse potential –reversal potential of I_{Ca}]), normalized (G/G_{max}), and plotted as a function of test potential. The voltage dependence of steady-state inactivation of Ca^{2+} currents was obtained using a standard two-test pulse. Briefly, cells were given a prepulse (E_{pre}) from -70 to 0 mV for 2 s, after which they were depolarized to a test potential (E_{test}) of 0 mV for 200 ms.

For intracellular Ca^{2+} concentration imaging experiments, dispersed β-cells were loaded with the acetoxymethyl form of the fluorescence Ca^{2+} indicator Fluo 4 (5 μM; 30min). Cells were perfused with an extracellular solution containing (in mM): 125 NaCl, 4.7 KCl, 1.2 KH_2PO_4, 1.2 $MgSO_4$, 5 $NaHCO_3$, 2 $CaCl_2$, 10 HEPES, and 2, 11 or 20 glucose adjusted to pH 7.4. Images were acquired using a Bio-Rad Radiance 2100 confocal system coupled to an inverted Nikon TE300 microscope equipped with a Nikon PlanApo (60X, NA = 1.4) oil-immersion lens, and analysed using NIH-ImageJ. For analysis, background-subtracted fluorescence signals were normalized by dividing the fluorescence (*F*) intensity at each time point by the resting fluorescence (F_0). Images were pseudo-colored using NIH-ImageJ.

Measurements of cyclic AMP concentration beneath the plasma membrane ($[cAMP]_{pm}$) was accomplished by total internal reflection fluorescence (TIRF) microscopy using a membrane anchored, truncated form of PKA-RIIβ with a CFP tag and YFP tagged PKA catalytic Cα subunit. When $[cAMP]_{pm}$ rises, Cα-YFP dissociates from the plasmalemmal-targeted regulatory subunit and translocates to the cytoplasm; the ratio of CFP-to-YFP fluorescence reflects the sub-membrane cAMP levels (Dyachok *et al*, 2008). Isolated islets cultured 2-5 days were infected with adenoviral constructs encoding the biosensor subunits. 24h after infection, the islets were allowed to attach to coverslips which were mounted in a chamber and superfused (0.3ml/min) with media containing (mM) 125 NaCl, 4.8 KCl, 1.3 $CaCl_2$, 1.2 $MgCl_2$, 25 HEPES, pH7.4. The islets were allowed to equilibrate 30min in basal medium containing 3mM glucose before stimulating with 20mM glucose or 5μM forskolin. The chamber was mounted on the stage of a Ti microscope with a 60X 1.45NA oil-immersion lens (Nikon), acquiring image pairs at 5s intervals with a back-illuminated EMCCD camera (DU-887; Andor Technology) controlled by MetaFluor software (Molecular Devices). CFP and YFP were excited by 458 and 514 nm light using an argon laser (Creative Laser Production). A filter

wheel with a mechanical shutter (Sutter Instruments) was used to select the appropriate wavelength and to block the excitation light between image captures. All imaging experiments were performed at 37°C.

Quantitative PCR was performed on mRNA obtained from islets cultured overnight in suspension. Approximately 100-150 islets were re-picked and mRNA was isolated using RNeasy spin columns with on column DNAse I treatment (Qiagen). Messenger RNA from liver or gastrocnemius muscle was isolated from fresh snap frozen tissue samples according to Qiagen protocols for RNeasy and RNeasy Fibrous Tissue kits with DNAse I treatment. Complementary DNA was generated using TaqMan reverse transcription reagents (Applied Biosystems). Quantitative real time PCR was performed using TaqMan gene expression assays for $Ca_V1.2\alpha1C$ (Mm00437917_m1), $Ca_V\beta3$ (Mm00432244_m1), Kir6.2 (Mm00440050_s1), SUR1 (Mm00803450_m1), GAPDH (4352932E) and TaqMan universal PCR master mix (4324018) with islet mRNA; skeletal muscle and liver samples were assayed using TaqMan primer/probe sets for G6Pase (Mm00839363_m1) and PEPCK (Mm01247058_m1), and GAPDH. Messenger RNA abundance was quantified by the $\Delta\Delta C_t$ method and GAPDH as the internal housekeeping transcript, and expressed as fold-WT.

Statistical Analysis and Molecular Modelling

All values are reported as mean±standard error (SEM) and the number of times the experiment was repeated (n) shown on the figures. Data were graphed and analysed using GraphPad Prism software (v5.0b). Integrated responses were calculated using the trapezoidal method using Prism with the basal values set as baseline. Statistical significance was determined by Student's t-tests, with p=0.05 as the significance level.

Models of the 2:1 PP2B-PIAIIIT complex were created using PDB ID 3LL8 (Li *et al*, 2012). An alternate asymmetric unit was selected that reflects the ability of the PIAIIIT peptide to

simultaneously contact two molecules of PP2B (Gold *et al*, 2011). All molecular representations were rendered using Pymol (Delano Scientific).

Supplementary References

Braun M, Wendt A, Buschard K, Salehi A, Sewing S, Gromada J, Rorsman P (2004) GABAB receptor activation inhibits exocytosis in rat pancreatic beta-cells by G-protein-dependent activation of calcineurin. *J Physiol* **559:** 397-409

Delmeire D, Flamez D, Hinke SA, Cali JJ, Pipeleers D, Schuit F (2003) Type VIII adenylyl cyclase in rat beta cells: coincidence signal detector/generator for glucose and GLP-1. *Diabetologia* **46:** 1383-1393

Dyachok O, Idevall-Hagren O, Sagetorp J, Tian G, Wuttke A, Arrieumerlou C, Akusjarvi G, Gylfe E, Tengholm A (2008) Glucose-induced cyclic AMP oscillations regulate pulsatile insulin secretion. *Cell Metab* **8:** 26-37

Efendiev R, Samelson BK, Nguyen BT, Phatarpekar PV, Baameur F, Scott JD, Dessauer CW (2010) AKAP79 interacts with multiple adenylyl cyclase (AC) isoforms and scaffolds AC5 and -6 to alpha-amino-3-hydroxyl-5-methyl-4-isoxazole-propionate (AMPA) receptors. *J Biol Chem* **285:** 14450-14458

Gold MG, Stengel F, Nygren PJ, Weisbrod CR, Bruce JE, Robinson CV, Barford D, Scott JD (2011) Architecture and dynamics of an A-kinase anchoring protein 79 (AKAP79) signaling complex. *Proc Natl Acad Sci USA* **108:** 6426-6431

Goldfine ID, German MS, Tseng HC, Wang J, Bolaffi JL, Chen JW, Olson DC, Rothman SS (1997) The endocrine secretion of human insulin and growth hormone by exocrine glands of the gastrointestinal tract. *Nat Biotechnol* **15:** 1378-1382

Hansotia T, Baggio LL, Delmeire D, Hinke SA, Yamada Y, Tsukiyama K, Seino Y, Holst JJ, Schuit F, Drucker DJ (2004) Double incretin receptor knockout (DIRKO) mice reveal an essential role for the enteroinsular axis in transducing the glucoregulatory actions of DPP-IV inhibitors. *Diabetes* **53:** 1326-1335

Hinke SA, Martens GA, Cai Y, Finsi J, Heimberg H, Pipeleers D, Van de Casteele M (2007) Methyl succinate antagonises biguanide-induced AMPK-activation and death of pancreatic beta-cells through restoration of mitochondrial electron transfer. *Br J Pharmacol* **150:** 1031-1043

Hohmeier HE, Mulder H, Chen G, Henkel-Rieger R, Prentki M, Newgard CB (2000) Isolation of INS-1-derived cell lines with robust ATP-sensitive K+ channel-dependent and -independent glucose-stimulated insulin secretion. *Diabetes* **49:** 424-430

Hoshi N, Langeberg LK, Scott JD (2005) Distinct enzyme combinations in AKAP signalling complexes permit functional diversity. *Nat Cell Biol* **7:** 1066-1073

Janjic D, Wollheim CB (1992) Islet cell metabolism is reflected by the MTT (tetrazolium) colorimetric assay. *Diabetologia* **35:** 482-485

Li H, Pink MD, Murphy JG, Stein A, Dell'Acqua ML, Hogan PG (2012) Balanced interactions of calcineurin with AKAP79 regulate Ca2+-calcineurin-NFAT signaling. *Nat Struct Mol Biol*: doi:10.1038/nsmb.2238

Logue JS, Whiting JL, Tunquist B, Sacks DB, Langeberg LK, Wordeman L, Scott JD (2011) AKAP220 organizes signaling elements that impact cell migration. *J Biol Chem*

Pamir N, Lynn FC, Buchan AM, Ehses J, Hinke SA, Pospisilik JA, Miyawaki K, Yamada Y, Seino Y, McIntosh CH, Pederson RA (2003) Glucose-dependent insulinotropic polypeptide

receptor null mice exhibit compensatory changes in the enteroinsular axis. *Am J Physiol Endocrinol Metab* **284:** E931-939

Postic C, Shiota M, Niswender KD, Jetton TL, Chen Y, Moates JM, Shelton KD, Lindner J, Cherrington AD, Magnuson MA (1999) Dual roles for glucokinase in glucose homeostasis as determined by liver and pancreatic beta cell-specific gene knock-outs using Cre recombinase. *J Biol Chem* **274:** 305-315

Tunquist BJ, Hoshi N, Guire ES, Zhang F, Mullendorff K, Langeberg LK, Raber J, Scott JD (2008) Loss of AKAP150 perturbs distinct neuronal processes in mice. *Proc Natl Acad Sci USA* **105:** 12557-12562

Weisenhaus M, Allen ML, Yang L, Lu Y, Nichols CB, Su T, Hell JW, McKnight GS (2010) Mutations in AKAP5 disrupt dendritic signaling complexes and lead to electrophysiological and behavioral phenotypes in mice. *PLoS One* **5:** e10325

Fig. S1

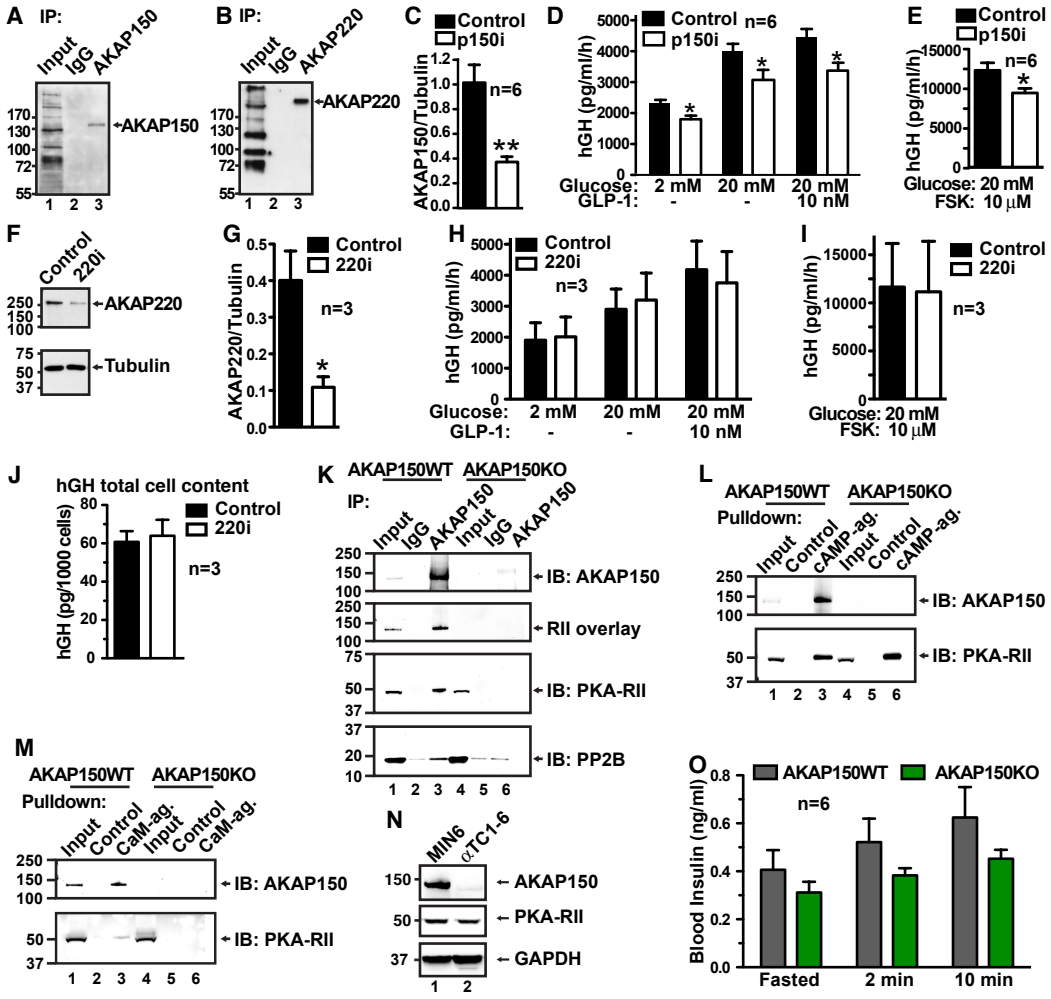
A
IP:
Input
IgG
AKAP150
AKAP150
170
130
100
72
55
1 2 3
B
IP:
Input
IgG
AKAP220
AKAP220
170
130
100
72
55
1 2 3
C
Control
p150i
AKAP150/Tubulin
n=6
**
D
Control
p150i
n=6
hGH (pg/ml/h)
Glucose: 2 mM 20 mM 20 mM
GLP-1: - - 10 nM
E
Control
p150i
n=6
hGH (pg/ml/h)
Glucose: 20 mM
FSK: 10 μM
F
Control
220i
AKAP220
Tubulin
250
150
100
75
50
37
G
Control
220i
AKAP220/Tubulin
n=3
H
Control
220i
n=3
hGH (pg/ml/h)
Glucose: 2 mM 20 mM 20 mM
GLP-1: - - 10 nM
I
Control
220i
n=3
hGH (pg/ml/h)
Glucose: 20 mM
FSK: 10 μM
J
hGH total cell content
Control
220i
n=3
hGH (pg/1000 cells)
K
AKAP150WT
AKAP150KO
IP:
Input
IgG
AKAP150
IB: AKAP150
RII overlay
IB: PKA-RII
IB: PP2B
1 2 3 4 5 6
L
AKAP150WT
AKAP150KO
Pulldown:
Input
Control
cAMP-ag.
IB: AKAP150
IB: PKA-RII
1 2 3 4 5 6
M
AKAP150WT
AKAP150KO
Pulldown:
Input
Control
CaM-ag.
IB: AKAP150
IB: PKA-RII
1 2 3 4 5 6
N
MIN6
αTC1-6
AKAP150
PKA-RII
GAPDH
1 2
O
AKAP150WT
AKAP150KO
n=6
Blood Insulin (ng/ml)
Fasted
2 min
10 min

Fig. S2

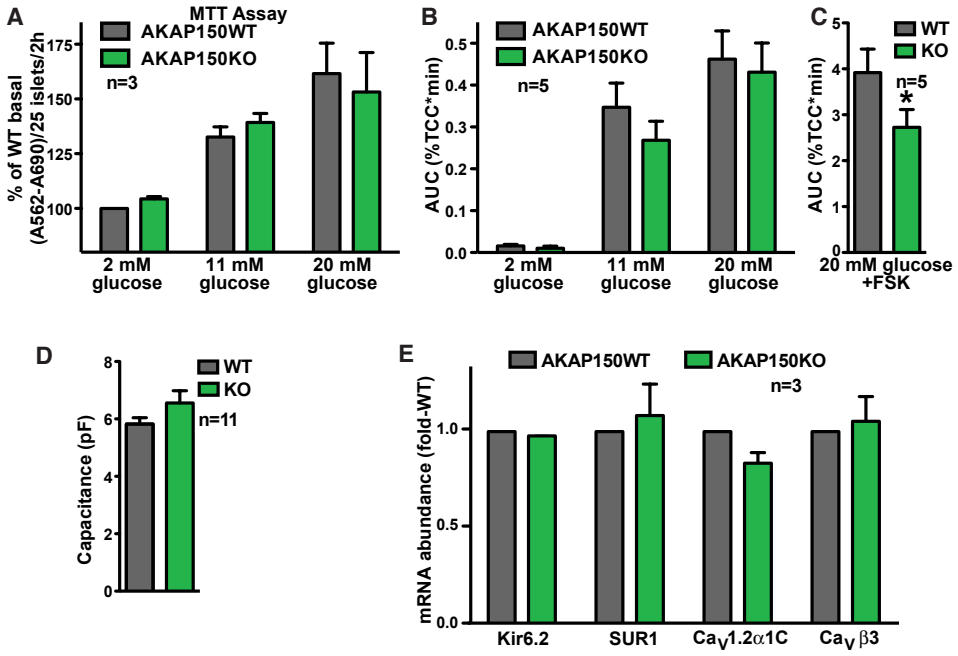
A
MTT Assay
AKAP150WT
AKAP150KO
n=3
% of WT basal
(A562-A690)/25 islets/2h
175
150
125
100
2 mM glucose
11 mM glucose
20 mM glucose
B
AKAP150WT
AKAP150KO
n=5
AUC (%TCC*min)
0.5
0.4
0.3
0.2
0.1
0.0
2 mM glucose
11 mM glucose
20 mM glucose
C
WT
KO
n=5
*
AUC (%TCC*min)
5
4
3
2
1
0
20 mM glucose +FSK
D
WT
KO
n=11
Capacitance (pF)
8
6
4
2
0
E
AKAP150WT
AKAP150KO
n=3
mRNA abundance (fold-WT)
1.0
0.5
0.0
Kir6.2
SUR1
CaV1.2α1C
CaV β3

Fig. S3

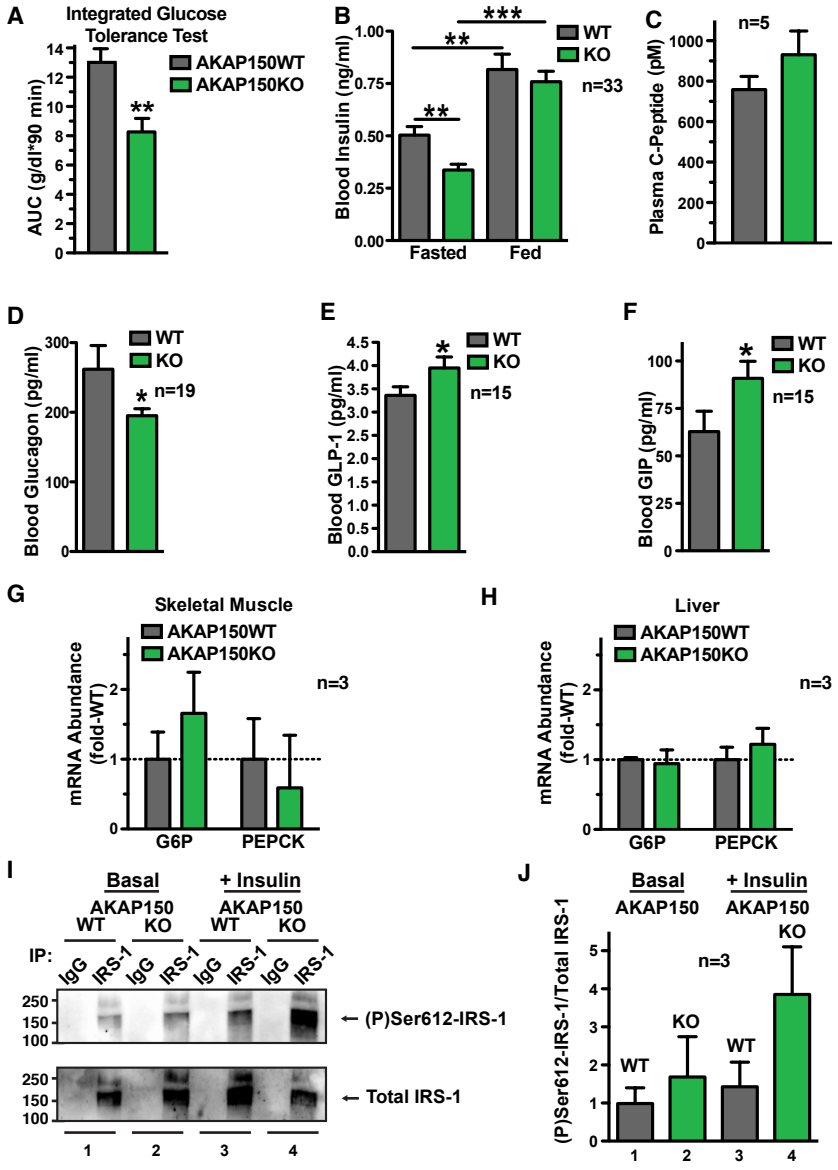
A
Integrated Glucose Tolerance Test
AKAP150WT
AKAP150KO
AUC (g/dl*90 min)
**
B
Blood Insulin (ng/ml)
WT
KO
n=33
**
***
Fasted
Fed
C
Plasma C-Peptide (pM)
n=5
D
Blood Glucagon (pg/ml)
WT
KO
n=19
*
E
Blood GLP-1 (pg/ml)
WT
KO
n=15
*
F
Blood GIP (pg/ml)
WT
KO
n=15
*
G
Skeletal Muscle
AKAP150WT
AKAP150KO
mRNA Abundance (fold-WT)
n=3
G6P
PEPCK
H
Liver
AKAP150WT
AKAP150KO
mRNA Abundance (fold-WT)
n=3
G6P
PEPCK
I
Basal
+ Insulin
AKAP150
WT
KO
IP:
IgG
IRS-1
← (P)Ser612-IRS-1
← Total IRS-1
1
2
3
4
J
Basal
+ Insulin
AKAP150
KO
n=3
(P)Ser612-IRS-1/Total IRS-1
WT
KO
WT
1
2
3
4

Fig. S4

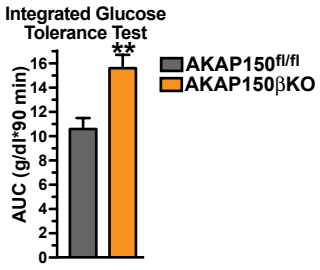
Integrated Glucose Tolerance Test
AUC (g/dl*90 min)
0
2
4
6
8
10
12
14
16
**
AKAP150fl/fl
AKAP150βKO

Fig. S5

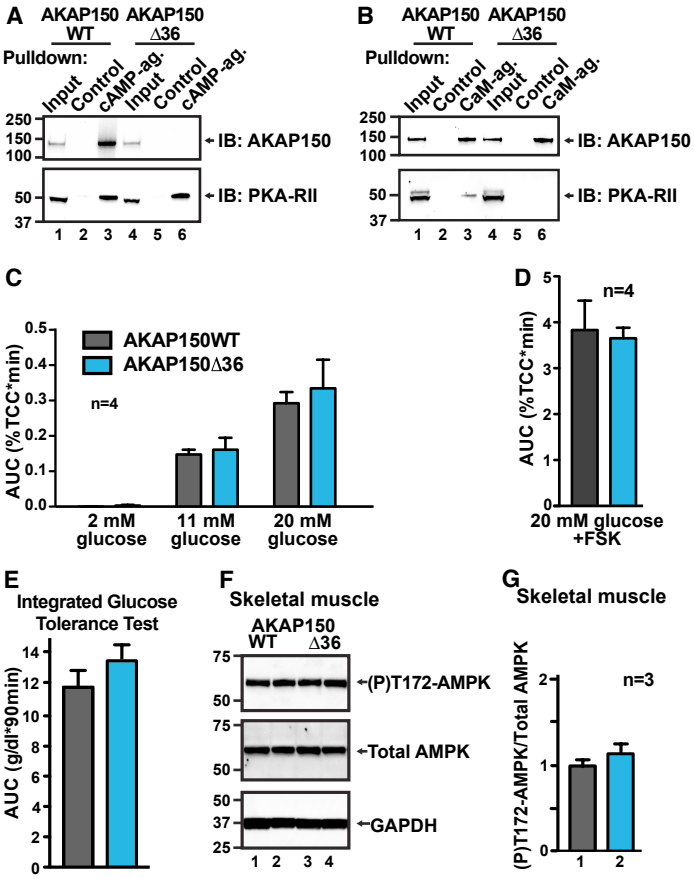
A
AKAP150 WT
AKAP150 Δ36
Pulldown:
Input
Control
cAMP-ag.
IB: AKAP150
IB: PKA-RII
B
CaM-ag.
C
AKAP150WT
AKAP150Δ36
n=4
AUC (%TCC*min)
2 mM glucose
11 mM glucose
20 mM glucose
D
n=4
20 mM glucose +FSK
E
Integrated Glucose Tolerance Test
AUC (g/dl*90min)
F
Skeletal muscle
(P)T172-AMPK
Total AMPK
GAPDH
G
Skeletal muscle
n=3
(P)T172-AMPK/Total AMPK

Fig. S6

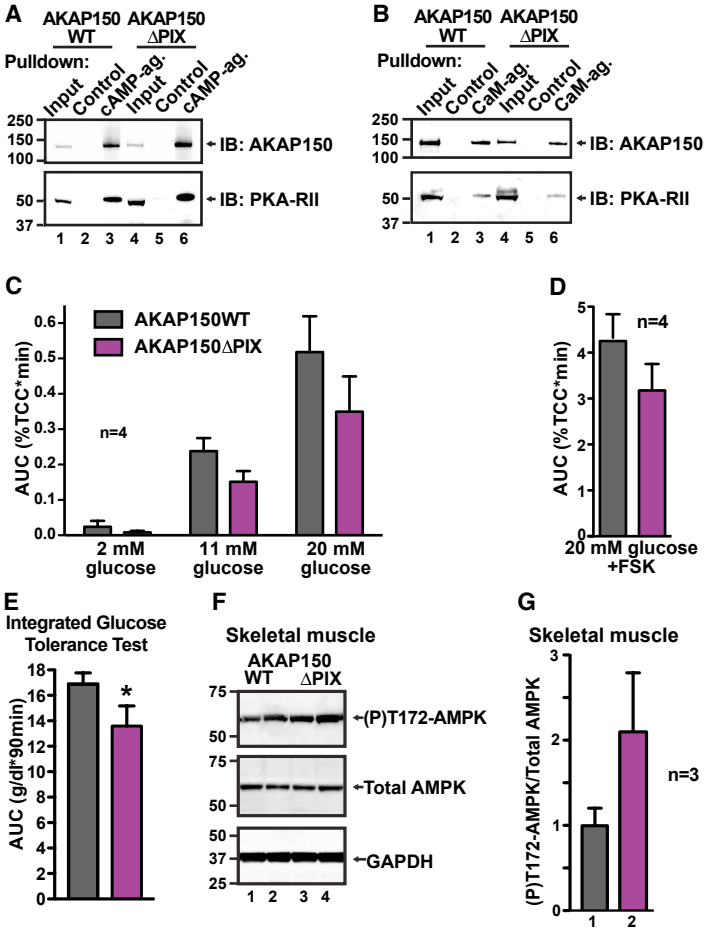
A
AKAP150 WT
AKAP150 ΔPIX
Pulldown:
Input
Control
cAMP-ag.
IB: AKAP150
IB: PKA-RII
B
CaM-ag.
C
AKAP150WT
AKAP150ΔPIX
n=4
AUC (%TCC*min)
2 mM glucose
11 mM glucose
20 mM glucose
D
20 mM glucose +FSK
E
Integrated Glucose Tolerance Test
AUC (g/dl*90min)
F
Skeletal muscle
(P)T172-AMPK
Total AMPK
GAPDH
G
(P)T172-AMPK/Total AMPK
n=3